# Multiresolution Transform based Denoising in Direction Finding

K.Gowri[1], P. Palnisamy[2]
Department of Electronics and Communication Engineering,
National Institute of Technology, Tiruchirappalli- 620 015

## ABSTRACT
In this paper, multi-resolution transforms based denoising followed by an improved method of Direction of Arrival (DOA) estimation is investigated. The predominant subspace method, Multiple Signal Classification (MUSIC) algorithm is very practical and efficient for direction of arrival estimation, but it fails to determine the direction at low Signal to Noise Ratio (SNR). The pre-eminence of MUSIC algorithm is used to upgrade the resolution of direction of arrival under adverse noisy situations. The noise is suppressed and thereby the gain of the received signal from sensors is improved by ridgelet transform and GHM (Geronimo J.S, Hardin D.P and Massopust P.R) multiwavelet transform based denoising. The simulation results of denoising and pseudo spectrum of the algorithm delivers improved performance in terms of root mean square error (RMSE), spectrum function, bias and gain. SNR, snapshots, array elements are the input parameters.

## General Terms
Direction of arrival, multiresolution transform based denoising

## Keywords
Multiresolution transform, ridgelet transform, GHM multiwavelet transform, DOA estimation, denoising, subspace methods

## 1. INTRODUCTION
Direction of Arrival (DOA) estimation has been a long-established problem in the field of sensor array processing. An achievement of accuracy is being an important issue in estimation. The applications of DOA estimation have received an attention in biomedical signal processing, target detection and so on [1]. Although the number of sensor elements and the samples of received signals, snapshots are less [4], the exploitation of subspace methods, Multiple Signal Classification (MUSIC) [2] and Estimation of Signal Parameters via Rotational Invariance Techniques (ESPRIT) [3] algorithm fail to resolve the signal efficiently. These algorithms depend on eigen value decomposition of the spatial covariance matrix. There are small angle errors in DOA estimation of ESPRIT than MUSIC was studied by Ottersten et al [5]. There should be a compromise between the trade-off factors such as accuracy, complexity, low SNR, coherence of sources, the number of sensors and the number of snapshots to obtain an efficient DOA estimation.

The detection and estimation of signals from noisy environment is a difficult process since many signals get impinged at sensors with unknown directions and amplitudes [6]. In this paper, an improved DOA estimation method for low SNR signal is proposed by denoising the signal array output using by 2D ridgelet transform and 2D-GHM multiwavelet transform. The SNR of the signals from the sensors are thus improved by multiresolution transforms. Wavelet Transform (WT) acts as the space-time localization of the signal and time-frequency coefficients are back transformed for denoising [7].

Wavelets are powerful tool to extract the information from noise with point singularities. The ridgelet transform is obtained by mapping point singularities using Radon transform and then the wavelet transform is applied, since wavelet transform fails to process line singularities [8]. One of the advantages of ridgelet transform is the original data can be processed to various scales and orientations [9]. Furthermore orthogonality, symmetry and a high order of approximation is preserved in multiwavelet with perfect reconstruction. The performance of multiwavelet bases is superior to other wavelet bases [10], [11]. Thresholding the multiresolution transformed coefficients using hard thresholding method gives denoising with better SNR.

In this paper, direction of arrival is estimated with accuracy is proposed using multiwavelet denoising since it gives preferred SNR improvement than other multiwavelet transforms. It achieves better in low SNR up to -30 dB whereas the method in [12] operates only up to -20dB. The performance of multiwavelet denoising outplays the ridgelet transform based denoising and is reported in literature [8]-[11]. In this study, the simulation results of DOA estimation using multiwavelet transform based denoising are compared with ridgelet transform based denoising. Denoising process supports the MUSIC algorithm to work in low SNR.

The organization of the paper is as follows. Section II outlines the data model. Section III describes the multiresolution transforms: ridgelet and multiwavelet transforms. In section IV, denoising technique is provided. Section V explains the MUSIC algorithm. Section VI describes the proposed work. Section VII illustrates the simulation results followed by a brief conclusion and future work.

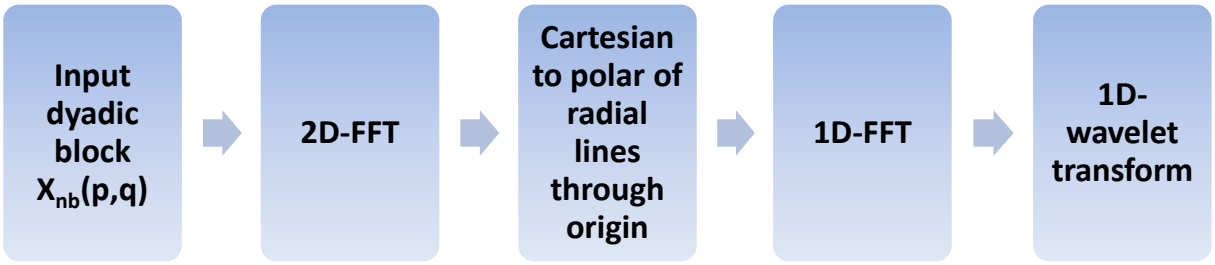


**Fig. 1. Block diagram of ridglet transform using 2D-FFT**

## 2. DATA MODEL

Consider an Uniform Linear Array (ULA) with sensors and they are equally spaced at $d = \lambda/2$. The number of sensors used for this problem formulation is M and if any narrow band sources $k$, $(M > k)$ with wavelength $\lambda$ impinging on the sensors at angles $(\theta_1, \theta_2, ..., \theta_k)$. Then the received signal in vector notation is given by

$$X(t) = A(t)S(t) + N(t) \quad for\ t = 1,2,...,L, \qquad (1)$$

where $L$ is the snapshots, $N(t)$ refers to an additive $M \times 1$ white Gaussian noise vector and it is assumed to be an uncorrelated and zero mean, $S(t)$ denotes the complex $k \times 1$ signal snapshots vector.

where $A$ is the steering matrix can be written as,

$$A = [a(\theta_1), a(\theta_2), ..., a(\theta_k)], \qquad (2)$$

with $a(\theta_k) = [1 \ \ e^{-j\frac{2\pi}{\lambda}d\sin(\theta_k)} \ .... \ e^{-j\frac{2\pi}{\lambda}d(M-1)\sin(\theta_k)}]^T$, (3)

Also assume that the signals and noise are uncorrelated with each other $(\forall_{i,j}; E[S_i N_j] = 0)$. The estimated covariance matrix, through snapshots can be obtained by,

$$\tilde{R} = \frac{1}{L}\sum_{i=1}^{L} XX^H = AR_{SS}A^H + R_{NN} \qquad (4)$$

where $R_{SS} \underline{\Delta}\underline{=} E[S(t)S(t)^H]$ represents spatial co-variance matrix and $R_{NN} = \sigma^2 I$, denotes variance of noise, $\sigma^2$ denotes the Gaussian noise vector variance, $E[.]$ stands for statistical expectation and $(.)$ denotes conjugate transposition.

## 3. MULTIRESOLUTION TRANSFORM

Multiresolution transform is an analysis tool to decompose the signal into space (time) - frequency domain. It performs onto the signal and it suits for different applications. It approximates the signals using inner product computation and scale and translation. It operates with the discrete set of samples of the signal and uses the dyadic wavelet sets.

### 3.1 RIDGELET TRANSFORM

The ridgelet transform decomposes the original signal to various scales and orientations, which represent different time frequency coefficients of the corresponding signal [13]. It compromises well with the line coefficients than point coefficients. This section reviews the Continuous Ridgelet Transform (CRT). Also it explains its similarity with other continuous transforms. The CRT of 1-D function $f(x)$ in $\Re^2$ is defined in [9],

$$CRT_f(\alpha, \beta, \vartheta) = \int_{\Re^2} \psi_{\alpha,\beta,\vartheta}(x)\, f(x)dx \qquad (5)$$

The mother wavelet is denoted by $\psi_{\alpha,\beta,\vartheta}(x)$, where $\alpha$ and $b$ is the scaling function and the translation function respectively. Ridgelet function is oriented at an angle $\vartheta$, where $\vartheta \in [0, 2\pi)$ and is constant along the line $x_1 \cos\vartheta + x_2 \sin\vartheta = const$. 1-D wavelet transform is applied to the signal in radon domain to obtain ridgelet transform. It is defined from 1-D wavelet type function $\psi(x)$ as,

$$\psi_{\alpha,\beta,\vartheta}(x) = \frac{1}{\alpha}\psi((x_1\cos\vartheta + x_2\sin\vartheta - b)/\alpha) \qquad (6)$$

If point specifications $(b, \vartheta)$ are replaced by $(b1, b2)$, then Continuous ridgelet transform is related to 2-D continuous wavelet transform The relationship between points and lines are dealt by 2D Radon transform and it is defined by,

$$R_f(\vartheta, t) = \iint f(x_1, x_2)\,\delta(x_1\cos\vartheta + x_2\sin\vartheta - t)dx_1dx_2 \qquad (7)$$

where $\delta$ is the Dirac distribution. The radon transform also satisfy the property,

$$R_f(\vartheta, t) = R_f(\vartheta + \pi, t) \qquad (8)$$

Applying 1-D wavelet transform to the radon coefficients is the ridgelet transform. This is also known as projections.

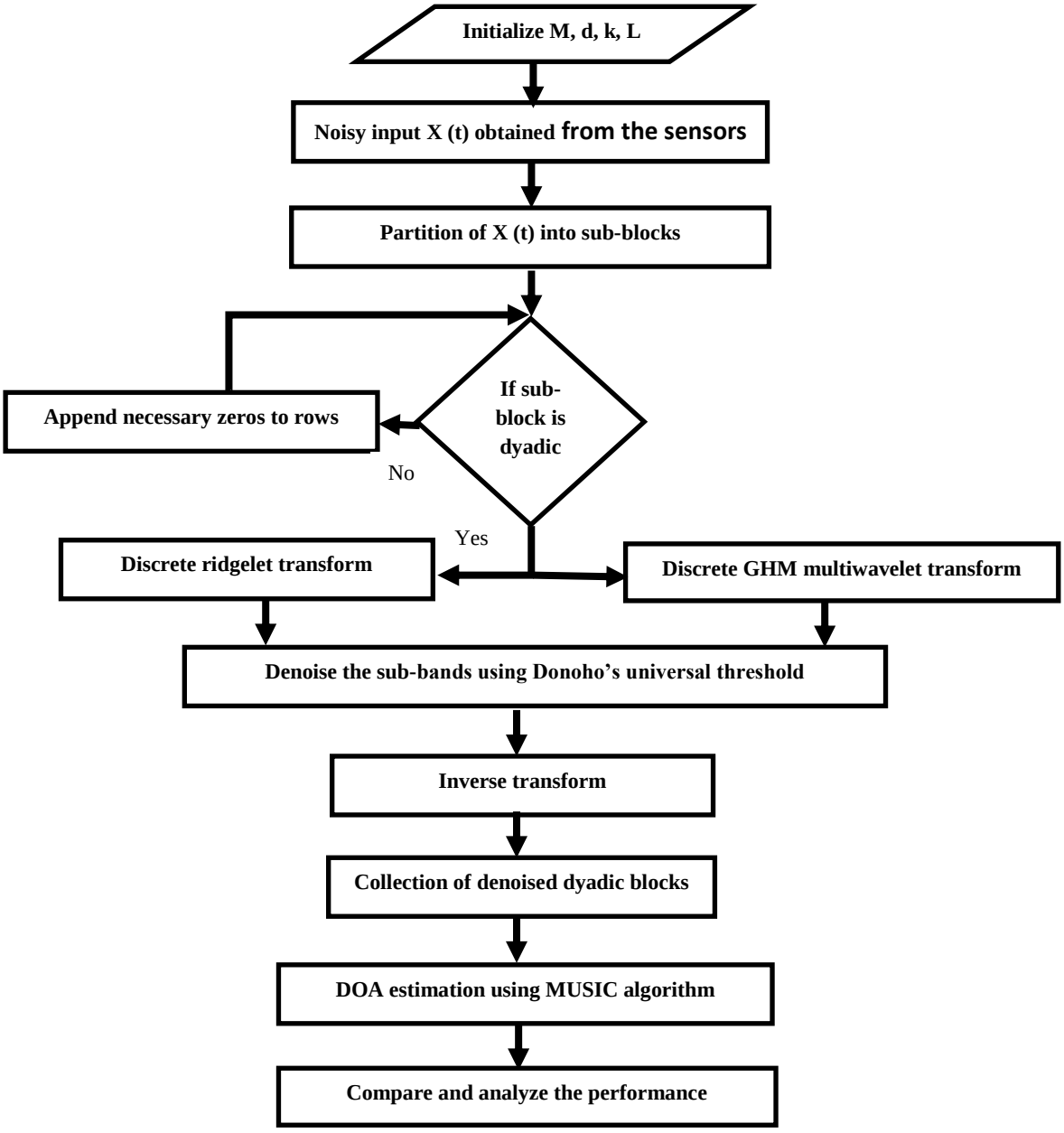


**Fig. 2. Flow chart for the proposed method**

The continuous ridgelet transform can be defined by,

$$CRT_f(\alpha,\beta,\vartheta) = \int_R \psi_{a,b}(t) R_f(\vartheta,t)dt \qquad (9)$$

ridgelet's cross section is like a mother wavelet. This makes ridgelet able to deal well with the line singularities [14]. Exploiting the projection slice theorem ridgelet transform can also obtained using Fourier transform instead of wavelet transform and is shown in fig.1

## 3.2 MULTIWAVELET TRANSFORM

GHM Multiwavelets are constructed by Geronimo et. al. and provide exceptional results in signal compression and denoising is given in the literature [15], [16]. The scaling function and the wavelet function in multiwavelets ought to be greater than one for analysis and synthesis of the signal [17]. The important properties such as orthogonality, compact support and so on can never more hold by uni-wavelets (with only one scaling and wavelet function, $\phi(t)$ and $\psi(t)$ simultaneously) [18].

Multiwavelets have w number of scaling functions and commonly w = 2 for multiwavelets. The scaling function and the wavelet function can be defined by vector notation as,

$$\phi(t) = [\phi_1(t) \;\; \phi_2(t)]^T \qquad (10)$$

$$\psi(t) = [\psi_1(t) \;\; \psi_2(t)]^T \tag{11}$$

where $\phi(t)$ and $\psi(t)$ is the multi-scaling function and multiwavelet function respectively. If $w = 1$, it matches to discrete or scalar wavelet [19]. The scaling and wavelet function for the scalar wavelet is given by,

$$\phi(t) = \sqrt{2} \sum_{m=-\infty}^{\infty} H_m \phi(2t - m) \tag{12}$$

$$\psi(t) = \sqrt{2} \sum_{m=-\infty}^{\infty} G_m \psi(2t - m) \tag{13}$$

For multiwavelets, the filters given in (12) and (13), $H_m$ and $G_m$ are $w \times w$ $(2 \times 2)$ matrices of low pass and high pass filter coefficients are given by,

$$H_m = \begin{bmatrix} h_0(2m) & h_0(2m+1) \\ h_1(2m) & h_1(2m+1) \end{bmatrix}, \tag{14}$$

$$G_m = \begin{bmatrix} g_0(2m) & g_0(2m+1) \\ g_1(2m) & g_1(2m+1) \end{bmatrix} \tag{15}$$

where the scaling filter sequence and the wavelet filter sequence are denoted by $h_m$ and $g_m$ respectively. They should satisfy $\sum_m h_m^2(n) = 1$ and $\sum_m h_m^2(n) = 1$ for $m = 0,1$.

A multiwavelet can preserve all the advantages of the wavelet [10]. Both the scaling and multiwavelet functions are symmetric and it offers superior performance compared with scalar wavelets in 2-D [20].

## 4. DENOISING USING UNIVERSAL THRESHOLD

Denoising is employed to recover the original signal from the noise corrupted signal. It smooths the signal by removing the high frequency components in the signal. In this paper, noise is assumed to be an additive Gaussian, which is uniformly distributed over the signal. Denoising can be done effectively through multiresolution transforms to eliminate additive noise is given in literature [12, 21, 22]. Denoising is done by applying the transform to the noisy signal which converts to orthogonal space, followed by thresholding and inverse transform to obtain the original domain. This is the estimate of the original signal.

The universal threshold proposed by Donoho [21] is given by,

$$T = \sigma \sqrt{2 \log(N_{Ts})} \tag{16}$$

where $N_{Ts}$ is the total number of coefficients in decomposition level and $\sigma$ denotes the standard deviation of Gaussian noise. The median of finest level transformed coefficients is denoted by $m_x$. Subsequently the standard deviation of Gaussian noise can be calculated from data $X$ can be given by,

$$\hat{\sigma} = \frac{m_x}{0.6745} \tag{17}$$

Calculation of standard deviation using (17) gives better estimate of the original signal for the hard threshold, if the number of samples is large. Thresholding must be done after decomposition of the input signal. Hard thresholding is used to denoised the signal in this paper and it is given by,

$$\hat{C}_{u,v} = \begin{cases} C_{u,v} & |C_{u,v}| \geq T, \\ 0 & |C_{u,v}| \geq T \end{cases} . \tag{18}$$

where $\hat{C}_{u,v}$ are the high frequency coefficients of transformed signal. When $\hat{C}_{u,v}$ is less than threshold $T$ it is replaced by zero, when it is greater than or equal to threshold $T$, it is contracted to zero according to fixed value. Then inverse transform is applied to obtain denoised estimate and is given by,

for Wavelet denoising, $\hat{f} = W^{-1}\hat{X}$, (19)

for Ridgelet denoising, $\hat{g} = CRT^{-1}\hat{X}$. (20)

At low signal to noise ratio, the universal threshold performs well for additive Gaussian noise. The energy compaction is high in ridgelet transform than wavelet transform, because ridgelet transform provides small number of coefficients at every level of decomposing.

## 5. MUSIC ALGORITHM FOR DOA ESTIMATION

Schmidt [2] proposed MUSIC algorithm for DOA estimation. To estimate the direction of arrival for multiple and uncorrelated multiple sources, MUSIC algorithm was introduced. Assume that the noise covariance matrix, $R_{NN}$ has a uniform power on its diagonal and the incident sources are uncorrelated. The spatial covariance matrix can be rewritten as,

$$R = E[X(t)X(t)^H] = AR_{SS}A^H + \sigma^2 I \tag{21}$$

where $R_{SS}$ is nonsingular and full rank matrix of $M \times M$ .MUSIC algorithm aids to estimate the desired arrival direction from $(\theta_1, \theta_2, ..., \theta_k)$ sources. The algorithm depends on eigen structure of the spatial covariance matrix. Signal and noise subspace matrices are obtained by decomposing covariance matrix and they are orthogonal to each other. The eigen decomposition is given by,

$$R = V\Lambda V^H = \begin{bmatrix} V_S & V_N \end{bmatrix} \begin{bmatrix} \Lambda_S & 0 \\ 0 & \Lambda_N \end{bmatrix} \begin{bmatrix} V_S{}^H \\ V_N{}^H \end{bmatrix} \quad (22)$$

where $V = [v_1, v_2, ..., v_k, v_{k+1}, ..., v_M]$ are eigen vectors, $V_S$ is signal subspace, $V_N$ is noise subspace and $\Lambda = diag[\lambda_1, \lambda_2, ..., \lambda_k, \lambda_{k+1}, ..., \lambda_M]$. The spectrum is maximized where noise and steering matrix are orthogonal to each other. Therefore MUSIC algorithm is the squares Euclidean norm of this vector. The MUSIC pseudo spectrum is, $P_{MUSIC}(\theta) = \dfrac{1}{a(\theta)^H V_N V_N{}^H a(\theta)}$ (23)

| | | | |
|---|---|---|---|
| $S_{1,1,1}$ | $S_{1,2,1}$ | $D^H{}_{1,1,1}$ | $D^H{}_{1,2,1}$ |
| $S_{1,1,2}$ | $S_{1,2,2}$ | $D^H{}_{1,1,2}$ | $D^H{}_{1,2,2}$ |
| $D^V{}_{1,1,1}$ | $D^V{}_{1,2,1}$ | $D^D{}_{1,1,1}$ | $D^D{}_{1,2,1}$ |
| $D^V{}_{1,1,2}$ | $D^V{}_{1,2,2}$ | $D^D{}_{1,1,2}$ | $D^D{}_{1,2,2}$ |

**Fig. 3. Decomposition of GHM multiwavelet transform**

## 6. THE PROPOSED DOA ESTIMATION USING MULTIWAVELET TRANSFORM BASED DENOISING

In this section, the description of the proposed method is provided. Firstly, the denoising of the received signal using ridgelet transform and GHM multiwavelet transform is discussed. The performance of denoising is analysed by gain. Secondly the denoised signal is used for DOA estimation. MUSIC algorithm is adopted for estimating sources and the results are provided in the next section. Consider an ULA of $M(M = 7)$ number of sensors, which are point sources. The signal through the sensors is deteriorated by Gaussian white noise $N(t)$. Using (1), (2) and (3), the signal $X(t)$ is given by,

$$X(t) = \begin{bmatrix} e^{-j\frac{\pi}{d}\sin\theta_1(0)} & \cdots & e^{-j\frac{\pi}{d}\sin\theta_k(0)} \\ \vdots & \ddots & \vdots \\ e^{-j\frac{\pi}{d}\sin\theta_1(M-1)} & \cdots & e^{-j\frac{\pi}{d}\sin\theta_k(M-1)} \end{bmatrix} S(t) + N(t) \quad (24)$$

$for\ t = 1,2,...,L$. The signal $X(t)$ is a two-dimensional array and thereby used for multiresolution based denoising. The data is partitioned into pieces of dyadic blocks $X_{nb}(p,q)$ where $nb$ is the number of blocks.

### 6.1 Ridgelet transform based denoising

1D-wavelet transform is applied to the Radon coefficients to obtain ridgelet transform. It is applied to the dyadic blocks $X_{nb}(p,q)$ using (7) and (9). Ridgelet transform can be performed for the input array, studied in [22]. Apply 2D-FFT to input dyadic blocks $X_{nb}(p,q)$ to polar, where the points fall on lines on a lattice going through the origin. Apply 1D-FFT on each line. Then apply 1D-wavelet transform to the slices of radon transform. Denoising is done with the output of the ridgelet transform, $R_X(\alpha,\beta,\vartheta)$ and hard thresholding in (18) is used to denoise the dyadic blocks. Compute inverse ridgelet transform to the denoised dyadic blocks and is written as,

$$X_{RD} = \sum_{nb} \int_0^\infty \int_{-\infty}^\infty \int_0^\infty |R_X(\alpha,\beta,\vartheta)| \frac{d\alpha}{\alpha^3} db \frac{d\theta}{4\pi} \quad (25)$$

The flow chart diagram for the proposed method is shown in fig.2.

### 6.2 GHM based denoising

The 2D-GHM multiwavelet transform is calculated by decomposing the noisy data using wavelet transform is obtained by applying either scaling or wavelet function in horizontal and vertical direction. After pre-filtering, the noisy 2D-dyadic data $X_{nb}(p,q)$ is replaced by four blocks. The approximate signal with coarsest level $J_0$ at resolution $2^{-m}$ is given by,

$$S_{m,l,k}(np,nq) = (< X_{nb}(p,q), \phi_{m,l,np}(p)\phi_{m,l,nq}(q) >) \quad (26)$$

The horizontal, vertical and diagonal details are given by,

$$D^H_{m,l,k}(np,nq) = (< X_{nb}(p,q), \psi_{m,l,np}(p)\phi_{m,l,nq}(q) >) \quad (27)$$

$$D^V_{m,l,k}(np,nq) = (< X_{nb}(p,q), \phi_{m,l,np}(p)\psi_{m,l,nq}(q) >) \quad (28)$$

$$D^D_{m,l,k}(np,nq) = (< X_{nb}(p,q), \psi_{m,l,np}(p)\psi_{m,l,nq}(q) >) \quad (29)$$

Sixteen sub-matrices of one level 2D-multiwavelet decomposition using (12) and (13) is shown in fig.3. The sub-matrices obtained by multiwavelet transform are denoised using Donoho's universal thresholding. This keeps the same coefficient value when coefficient greater than $T$ and kills when less than $T$ using (16) - (18). Reconstructed 2D data is obtained by applying inverse transformation of sub-bands and post filtering of the dyadic blocks. Collection of the dyadic blocks give denoised signal $X_{MWT}$, which can be used for DOA estimation.

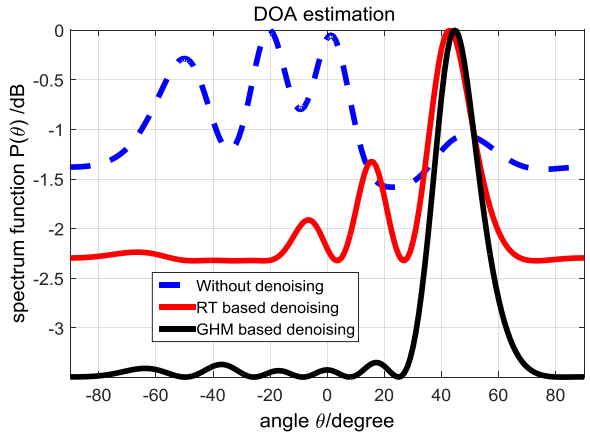


**Fig 4. DOA estimation at $\theta = 45^0$, SNR= -30dB and L=640**

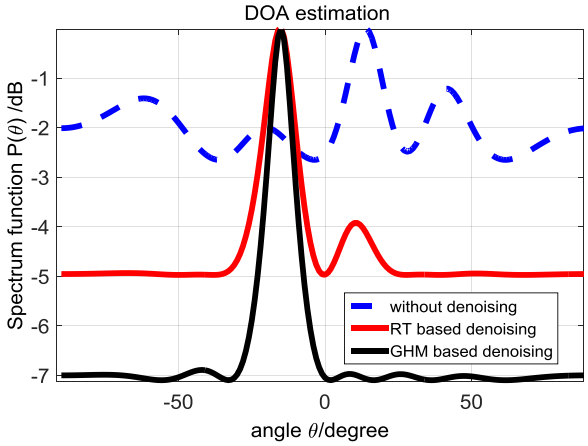


**Fig 5. DOA estimation at $\theta = -15^0$, SNR= -20dB and L=640**

## 6.3 DOA estimation

Compare the performance of the denoising using metric gain. Compute $M \times M$ correlation matrix using denoised signal $X_{MWT}$, assuming sources are independent and noise is uncorrelated. If $M > k$ the matrix $AR_{SS}A^H$ is singular $(\det[AR_{SS}A^H] = 0)$. $M$ Dimensional vector subspace is partitioned into signal subspace $V_S$ and noise subspace $V_N$ using eigen decomposition. MUSIC algorithm searches through all angles and when $\theta = \theta_i, i = 1,2,...,k$ it exhibits a peak value. The spatial spectrum is plotted using (23).

## 7. RESULTS AND DISCUSSION

DOA estimations are simulated using MATLAB tool. In this section we describe about DOA estimation using ridgelet and multiwavelet transform based denoising. The proposed method describes the DOA estimation of the noisy input signal received at the sensor output by removing the noisy to obtain the accurate and high resolution performance. To accomplish this, multi-resolution transforms: 2D-multiwavelet and 2D-ridgelet transform is used and simulation results are noted in this paper.

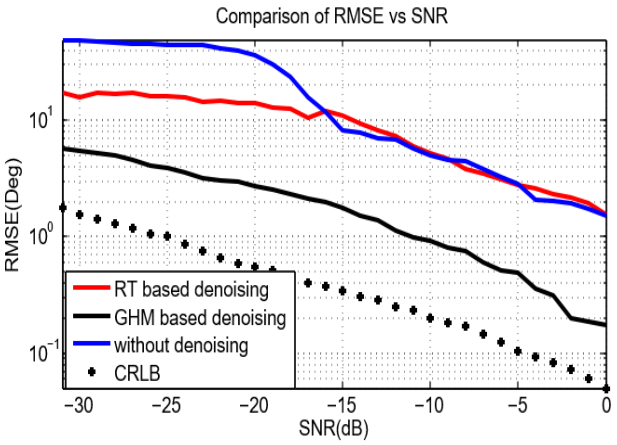


**Fig 6. RMSE versus SNR**

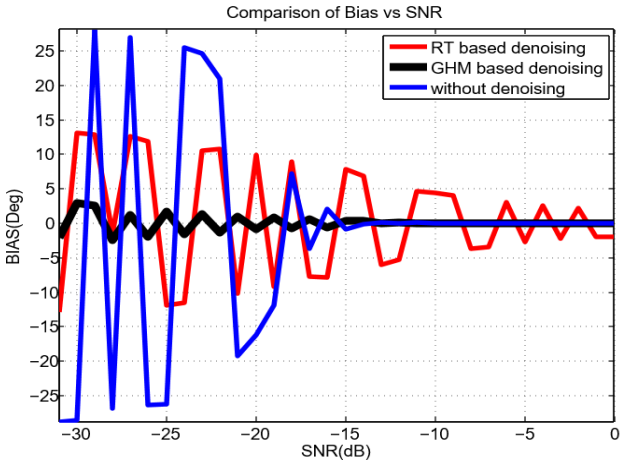


**Fig 7. Bias versus SNR**

The performance measures like Gain and Root Mean Square Error (RMSE) are studied for various values of input SNR, angles and inter-element spacing, $d$. A uniform linear array of $M = 7$ sensors at $d = \lambda/2$ and the number of narrow band signals $k = 1$ is considered in our simulation results. The noise assumed in this proposed work is zero mean, additive white Gaussian. The empirical SNR gain function $G_X$ [12], is defined as,

$$G_X = (SNR)_I - (SNR)_O \tag{30}$$

The input SNR is, $(SNR)_I = \left( \frac{E[\|S\|]^2}{E[\|S - X\|]^2} \right)$ (31)

The output SNR is, $(SNR)_O = \left( \frac{E[\|S\|]^2}{E[\|S - \hat{S}\|]^2} \right)$ (32)

Where $S$ is the original signal, $X$ is noise corrupted signal at sensors, $\hat{S}$ is the denoised signal using multiresolution transform.

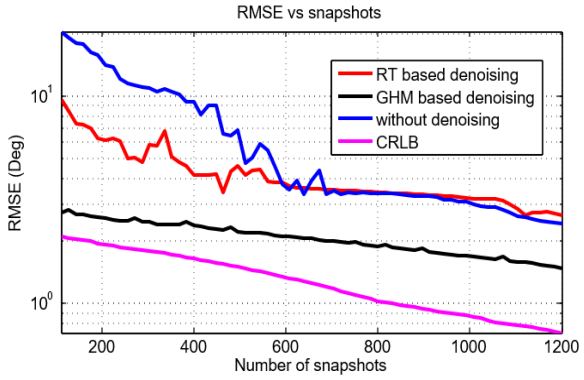


**Fig 8. RMSE versus snapshots**

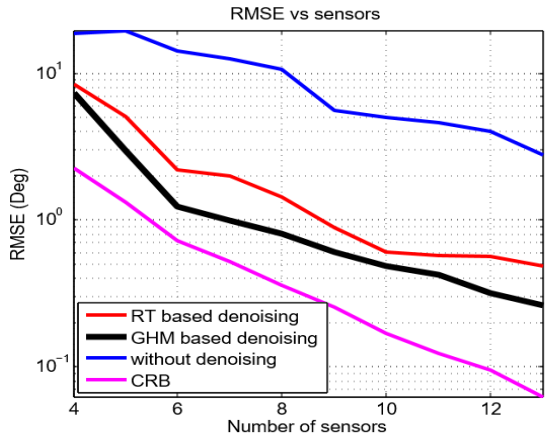


**Fig 9. RMSE versus sensors**

The Gain value 3.0515dB is calculated by averaging over 500 Monte-Carlo simulations for different values of SNR.

To calculate the performance of the proposed method, the angle of arrival is set to $45^0$, the input signal to noise ratio is $-30dB$. The inter element spacing is set as half a wavelength for all experiments. The noise is additive white Gaussian noise with snapshots, $L=640$. Fig. 4shows the DOA estimation of angle $45^0$ for $7$ sensors. The evaluation is done by comparing the performance of the proposed GHM multiwavelet transform based denoising method with ridgelet transform and undenoised signal based DOA. Fig. 4 illustrates, in the low SNR environment the DOA estimation by GHM based denoising is accurate with high resolution. Fig. 5 displays the simulation result for the case of $\theta=-15^0$ , with $640$ snapshots at input $SNR=-20dB$. Thus DOA estimation by GHM based denoising performs well when compared with the performance of RT based denoising. This simulation result also provides high accuracy and is done with 7 numbers of sensors. It distinguishes well and provides satisfactory result on DOA estimation.

The performance benchmark, Root Mean Square Error (RMSE) is calculated with respect to $30^0$ and $63^0$. The number of snapshots used in this simulations is $640$, the SNR ranges from $-30dB$ to $0dB$ and $M=7$. The average RMSE of the signal impinged on the sensors is used for statistical DOA estimation precision evaluation is defined by,

$$RMSE=\sqrt{\frac{1}{N_S}\sum_{i=1}^{N_S}(\theta-\hat{\theta})^2} \qquad (33)$$

where $N_S$ is the number of trials, $\theta$ is true angle and $\hat{\theta}_i$ is the estimate DOA of $i^{th}$ sample. Fig. 6 evaluates the denoising performance in terms of RMSE of DOA estimation by simulation. The snapshots of received data are $640$ and the number of independent trials is $500$. The angle $\theta$ was fixed at $30^0$ and furthermore SNR varies from $-30dB$ to $0dB$. Fig. 7 shows the corresponding bias result. From Fig. 6 and 7, GHM based denoising exhibits superior performance than RT based denoising and undenoised received signal. For reference, Cramer Rao Lower Bound (CRLB) is provided in this simulation.

The performance of the proposed method shown in Fig. 8 is evaluated by RMSE versus number of snapshots. The snapshots are varied with a step size of $16$ from $112$ to $1200$ at $SNR=-20dB$. The number of independent trials used is $500$. Again, the proposed method shows the better performance than other methods.

The RMSE of DOA estimation by GHM based denoising outperforms RT based denoising and undenoised signal and is shown in Fig. 9. This simulation was done via $500$ snapshots and the input SNR is $-17dB$. The angle was fixed at $12$ along with $500$ independent trials. Fig. 9 interprets the performance of the proposed method through RMSE versus sensors.

The resolving capablity of the proposed approach was verified with two sources (k=2) through simulations. Simulations acheive excellent results as input SNR varies upto $-29\,dB$, moreover sources were fixed at $\theta=10^o$ and $\theta=30^o$. GHM based estimation performs good for low SNR. This is reported in figure 10 and the input SNR used for this simulation is $-29\,dB$.

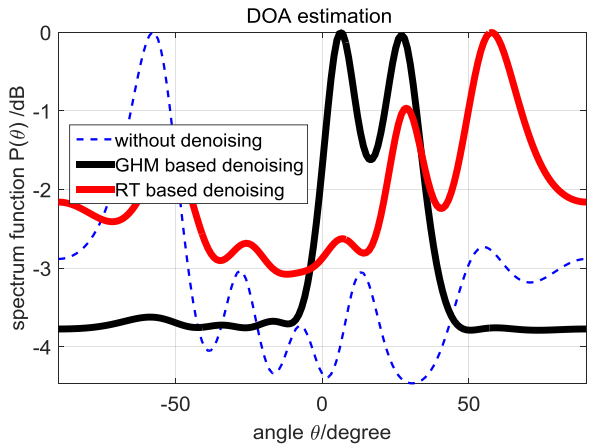


**Fig 9. DOA estimation of two sources at $\theta = 10^0$ , $\theta = 30^0$, L=640, SNR= -19dB**

## 8. CONCLUSION

This paper investigated the accuracy of available Direction of Arrival algorithms. To increase the performance, multi-resolution transforms- multiwavelet Transform and ridgelet transform are proposed for denoising. The simulation results demonstrate in low SNR ( $SNR = -30dB$ ), GHM based denoising estimates accurate DOA, where ridgelet transform based denoising fails. It is shown that, especially in low SNR, GHM based DOA estimation increases the accuracy and reduces the RMSE of the DOA estimates when compared to ridgelet based estimation. The future work will include denoising using Multi-resolution transform to reduce the number of sensors, complexity and resolve more and close signals. It is believed that further improvements in performance will be achieved by selecting an appropriate estimating algorithm. Simulation results support the effectiveness of the proposed method.

## 9. REFERENCES

[1] Harry. L. Van Trees, 2002. Detection, Estimation and Modulation Theory. Optimum Array Processing, Wiley, 1-13.

[2] Ralph. O. Schmidt, 1986. Multiple Emitter Location and Signal Parameter Estimation, IEEE Trans. on Antennas and Propagation, 34(3), 276–280.

[3] Roy. R and Kailath. T, 1989. Estimation of Signal Parameters via Rotational Invariance Techniques. IEEE Trans. on Acoust., Speech, Signal Processing, 60(12) 984–995.

[4] Wei. X, Yuan. Y and Ling. Q, Dec 2012. DOA Estimation using a Greedy Block Coordinate Descent Algorithm. IEEE Trans. Signal Processing, 60(12), 6382–6394.

[5] Ottersten. B, Viberg.M and Kailath. T, 1991. Performance Analysis of the Total Least Squares ESPRIT Algorithm. IEEE Transactions on Signal Processing, 39(5), 1122–1135.

[6] Capon. J, 1979. Maximum Likelihood Spectral Estimation. Nonlinear Methods Spectral Anal., 34, 155–179.

[7] Zhang. L, Dong. W, Zhang. D and Shi. G, 2010. Two-Stage Image Denoising by Principal Component Analysis with Local Pixel Grouping. Pattern Recognition, 43, 1531–1549.

[8] Do. M. N, Vetterli. M, Jan. 2003. The Finite Ridgelet Transform for Image Representation. IEEE Transactions on Image Processing, 12(1), 16–28.

[9] Chen. G. Y and Kegl. B, 2007. Image Denoising with Complex Ridgelets. Pattern Recognition, 40, 578–585.

[10] Wang. H, Peng J and Wu W, Oct. 2002. Fusion Algorithm for Multisensory Images Based on Discrete Multiwavelets Transform. IEEE Proc. Vis. Image signal Processing, 149(5), 283–289.

[11] Strang. G, Strela. V, 1995. Short Wavelets and Matrix Dilation Equations. IEEE Trans. signal Processing, 43, 108–115.

[12] Sathish. R and Anand. G. V, 2014 .Wavelet Array Denoising for Improved Direction of Arrival Estimation. Bangalore: IISc, Technical Report Tr-PME-2003-2014. DRDO-IISc Program on Mathematical Engineering.

[13] Candes. E. J, 1998. Ridgelets: Theory and Applications. Ph.D Dissertation: Dept. Statistics, Stanford Univ., Stanford, CA,

[14] Yang. S, Wang. M and Jiao. L, 2007. Geometrical Multi-Resolution Network Based on Ridgelet Frame. Signal Processing,Elsevier, 87, 750–761.

[15] Geronimo. J. S, Hardin. D. P. and Massopust P. R., 1994. Fractal Functionsand Wavelet Expressions based on Several Scaling Functions. J. Approx. Theory, 78, 373–409.

[16] Strela. V, Heller. P. N, Strang. Topiwala. G, P and Heil. C, 1999. The Application of Multiwavelet Filter Banks to Image Processing. IEEE Transactions on Image Processing, 8, 548–563.

[17] Tham J. Y, shen. L, Lee S. L and Tan H. H, Feb. 2000. A General Approach for Analysis and Application of Discrete Multiwavelet Transforms. IEEE Trans. Signal Processing, 48(2), 457–464.

[18] Xinxing. Y and Licheng. J, Jan.1999. Adaptive Multiwavelet Prefilter. Electronic letters, 35(1), 11–13.

[19] Serdean. C. V, Ibrahim. M. K, Moemeni. A and Al-akaidi M. M, 2007. Wavelet and Multiwavelet Watermarking. IET Image Processing, 1( 2), 223–230.

[20] Jiao. L, Pan. J. and Fang. Y, Sep.2001. Multiwavelet Neural Network and its Approximation Properties. IEEE Trans. Neural Networks, 12(5), 1060–1066.

[21] Donoho. D. L and Johnstone. I. M, 1995. Denoising by Soft Thresholding. IEEE Transactions on Information Theory, 41, 613–627.

[22] Starck. J. L, Candes E. J and Donoho D. L, June 2002. The Curvelet Transform for Image Denoising. IEEE Transactions on Image Processing, 11(6), 670–684.